Chin. J. Astron. Astrophys. Vol. 1, No. 3, (2001) 200–212
(http://www.chjaa.org or http://chjaa.bao.ac.cn)

Chinese Journal of
Astronomy and
Astrophysics

A DWT Power Spectrum Analysis of PSCz Galaxies

Xiao-Hu Yang[1,2] ⋆, Long-Long Feng[1,2] and Yao-Quan Chu[1,2]

[1] Center for Astrophysics, University of Science and Technology of China, Hefei 230026
[2] National Astronomical Observatories, Chinese Academy of Science, Beijing 100012

Received 2000 November 30; accepted 2001 April 9

Abstract The power spectrum estimator based on the Discrete Wavelet Transformation (DWT) is applied to detect the clustering power in the IRAS Point Source Catalog Redshift Survey (PSCz). Comparison with mock samples extracted from N-body simulation shows that the DWT power spectrum estimator could provide a robust measurement of banded fluctuation power over a range of wavenumbers $0.1 \sim 2.0\,h\,\mathrm{Mpc}^{-1}$. We have fitted three typical CDM models (SCDM, τCDM and ΛCDM) using the Peacock-Dodds formula including non-linear evolution and redshift distortion. We find that, our results are in good agreement with other statistical measurements of the PSCz.

Key words: large-scale structure of Universe — Methods: N-body simulations

1 INTRODUCTION

Accurate measurement of the power spectrum of galaxies has been an essential issue in the study of large scale structure of the universe. The shape and amplitude of power spectrum contain information on the nature of dark matter and the relative density of dark matter to baryons. The power spectrum of galaxies has been estimated from a number of redshift surveys, notably the CfA redshift survey (Park et al. 1994), the QDOT survey (Feldman, Kaiser & Peacock 1994), the 1.2 Jy IRAS survey (Fisher et al. 1993), the Stromlo-APM redshift survey (Tadros & Efstathiou 1996), and the Las Campanas survey (Lin et al. 1996). Also, the real-space power spectrum has been extracted from the APM Galaxy Survey (Baugh & Efstatiou 1993, 1994) by inversion of both the angular correlation and 2-D power spectrum.

Standard method of power spectrum analysis is based on Fourier decomposition of the density field in discrete plane wave modes. However, this method has several weaknesses, among which a critical problem is that the basis functions of Fourier expansion are not orthonormal over a finite non-periodic volume, which leads to the estimated power spectrum being a convolution of the real power spectrum and a survey-geometry dependent window function. Also, there is an ambiguity in the optimal number of modes included in the band-average power estimation. Moreover, the nonlinear mode-mode coupling on small scales may lead to the reduction of

⋆ E-mail: xhyang@mail.ustc.edu.cn

independent modes and thus increasing errors in the power spectrum estimation.

An alternative method of power spectrum analysis is to use multiresolution analysis based on the Discrete Wavelet Transformation (DWT). Unlike the Fourier bases which are inherently nonlocal, the DWT allows for an orthogonal and complete projection on modes localized in both physical and scale spaces, and makes possible a multiscale resolution adaptive to the wavelength to be studied. Moreover, the DWT estimator can fully avoid the alias effect present in usual binning schemes, which limits us to probe the density fluctuations on small scales. The general method of DWT power spectrum analysis presented by Fang & Feng (2000) was applied to the measurement of the DWT power in an observed sample, the Las Campanas Redshift Survey (Yang et al. 2000).

This paper is to perform the DWT power spectrum analysis of the PSCz Redshift Survey. The measurement based on Fourier estimator has been presented by Sutherland et al. (1999). So far, a variety of statistical methods have been applied to this samples, e.g., the topology analysis of the density field (Canavezes et al. 1998), dipole estimation (Rowan-Robison et al. 2000), reconstruction of the peculiar velocity field (Branchini et al. 1999), the redshift distortion analysis (Tadros et al. 1999; Hamilton et al. 2000).

The paper is organized as follows: The PSCz redshift survey is described in Section 2. In Section 3, we give a brief review of the power spectrum estimator in terms of DWT formalism. In Section 4, the DWT power spectrum estimators are tested using mock catalogues extracted from N-body simulations. An analysis of the PSCz catalogue and a comparison with the parameterized cosmological models are made in Section 5. Our conclusions are given in Section 6.

2 THE PSCz GALAXIES

The IRAS Point Source Catalog Redshift Survey (PSCz) is the largest all-sky survey in existence (Saunders et al. 2000). It covers 84% of the sky with a total of about 15000 redshifts. This, together with its careful consideration of mask, selection criteria and uniformity, makes PSCz the finest available galaxy redshift survey for measuring the DWT power spectrum.

As the survey depth of the PSCz is not very large (with median redshift $8500\,\mathrm{km\,s^{-1}}$), the redshift-distance relation could be approximated by the Hubble law. We first consider the magnitude-limited samples of the PSCz, in which we need to weight the galaxies by the inverse of the selection function. So the brightest and rarest galaxies at large distances have large weighting, which will introduce large shot noise term and sample uniformity problem. To measure the PSCz DWT power spectrum precisely, we use the high-latitude PSCz sky mask and further restrict the galaxies in region $|b| > 20^\circ$. Two samples with distance $10 < r < 75\,h^{-1}$Mpc (FLUX1, hereafter) and $10 < r < 150\,h^{-1}$Mpc (FLUX2, hereafter) are considered separately.

The selection functions we adopt here are those of Saunders et al.(2000), for which they give both non-parametric and parametric forms. The double power-law form selection function is

$$\psi(r) = \psi_* \left(\frac{r}{r_*}\right)^{-\alpha} \left[1 + \left(\frac{r}{\beta r_*}\right)^{\gamma}\right]^{\frac{-\beta}{\gamma}}, \tag{1}$$

and the parameters are $\psi = 0.0077$, $\alpha = 1.82$, $r_* = 86.4$, $\gamma = 1.56$, $\beta = 4.43$.

We also select volume-limited samples from the PSCz catalogue for the DWT power spectrum analysis, in which we use the high-latitude PSCz sky mask and restrict to distance

$10 < r < 75\,h^{-1}$Mpc (VOLUME1, hereafter) and $10 < r < 150\,h^{-1}$Mpc (VOLUME2, hereafter). The two volume-limited samples contain 1865 and 1525 galaxies each.

3 ESTIMATOR OF THE DWT POWER SPECTRUM

The galaxies in the universe are generally assumed to be distributed as a Poisson point process with an intensity $n_g(\boldsymbol{x})$ modulated both by a selection function $\bar{n}_g(\boldsymbol{x})$ and fluctuation $\delta(\boldsymbol{x})$ in the underlying matter distribution, $n_g(\boldsymbol{x}) = \bar{n}_g(\boldsymbol{x})(1+\delta(\boldsymbol{x}))$. Using the discrete wavelet transformation (Fang & Thews 1998), we realize a decomposition of the density fluctuation by projection onto the multiresolution space spanned by a wavelet basis $\{\psi_{\boldsymbol{j},\boldsymbol{l}}(\boldsymbol{x})\}$

$$\tilde{\epsilon}^{\boldsymbol{l}}_{\boldsymbol{j}} = \int \Big[\frac{n_g(\boldsymbol{x})}{\bar{n}_g(\boldsymbol{x})} - 1\Big]\psi_{\boldsymbol{j},\boldsymbol{l}}(\boldsymbol{x})d\boldsymbol{x}\,, \tag{2}$$

which defines the wavelet coefficient $\tilde{\epsilon}^{\boldsymbol{l}}_{\boldsymbol{j}}$ on the scale $\boldsymbol{j} = \{j_1, j_2, j_3\}$ localized at the position $\boldsymbol{l} = \{l_1, l_2, l_3\}$. We embed the galaxies in a box of side L and make periodic extension of the density field. Thus we have $2^{j_1+j_2+j_3}$ wavelet coefficients $\tilde{\epsilon}^{\boldsymbol{l}}_{\boldsymbol{j}}, l_i = 0...2^{j_i-1}, i = 1,2,3$ at the scale $\boldsymbol{j}$.

We define covariance matrix $\boldsymbol{C}_{\boldsymbol{j}}$ at scale $\boldsymbol{j}$ by

$$C^{\boldsymbol{ll'}}_{\boldsymbol{j}} = \tilde{\epsilon}^{\boldsymbol{l}}_{\boldsymbol{j}} \cdot \tilde{\epsilon}^{\boldsymbol{l'}}_{\boldsymbol{j}}\,. \tag{3}$$

Accordingly, the estimator of fluctuation power on the $\boldsymbol{j}$ scale defined by Eq. (2) is obtained by averaging over the $2^{j_1+j_2+j_3}$ measurements in the disjoint volume elements,

$$I^2_{\boldsymbol{j}} = \frac{1}{2^{j_1+j_2+j_3}}\mathrm{tr}\boldsymbol{C}_{\boldsymbol{j}} = \overline{\sum_{\boldsymbol{j}}}|\tilde{\epsilon}^{\boldsymbol{l}}_{\boldsymbol{j}}|^2\,, \tag{4}$$

where the normalized summation notation for average in three dimensions $\overline{\sum_{\boldsymbol{j}}} = \prod_{i=1}^{3}\frac{1}{2^{j_i}}\sum_{l_i=0}^{2^{j_i}-1}$ is used.

The power estimator Eq. (4) includes two contributions one from the signal $S_{\boldsymbol{j}}$ and one from shot noise $N_{\boldsymbol{j}}$. The signal power is

$$\bar{S}_{\boldsymbol{j}} = \frac{1}{2^{j_1+j_2+j_3}}\mathrm{tr}\boldsymbol{S}_{\boldsymbol{j}} = \sum_{\boldsymbol{n}} W_j(\boldsymbol{n})P(\boldsymbol{n})\,, \tag{5}$$

with the filter

$$W_{\boldsymbol{j}}(\boldsymbol{n}) = \prod_{i=1}^{3}\frac{1}{2^{j_i}}|\hat{\psi}(n_i/2^{j_i})|^2\,. \tag{6}$$

The function $\hat{\psi}(n)$ is the Fourier transform of the basic wavelet $\psi(x)$, where n labels the wavenumber by $k = 2\pi n/L$. $\hat{\psi}(n)$ is orthogonal to the monopole, i.e., $\hat{\psi}(0) = 0$ and is localized in wavenumber space. For the Daubechies 4-wavelet, $|\hat{\psi}(n)|^2$ has symmetrically distributed peaks with respect to $n = 0$. The first highest peaks are non-zero in two narrow ranges centered at $n = \pm n_p$. Because of $\int W_j(\boldsymbol{n})d\boldsymbol{n} = 1$, $W_j(\boldsymbol{n})$ plays the role of window function in the estimator Eq. (5). Obviously, $\bar{S}_j$ represents band averaged power spectrum in $\log n$. For a given $\boldsymbol{j}$, the corresponding central frequency in the band power is (Pando & Fang 1998)

$$\log(n_{\boldsymbol{j}}) = (\log 2)|\boldsymbol{j}| + \log n_p, \quad |\boldsymbol{j}| = \sqrt{j_1^2 + j_2^2 + j_3^2}\,. \tag{7}$$

The band width in $\log n$ is kept constant, i.e., $\Delta \log n = \Delta n_p/n_p$, in which Δn_p is defined by equal area under $|\psi(n)|^2$, i.e., $|\psi(n_p)|^2 \Delta n_p = 1/2$, the one half factor arises from the two symmetrical peaks.

The noise term is

$$\bar{N}_{\boldsymbol{j}} = \frac{1}{2^{j_1+j_2+j_3}} \mathrm{tr} \boldsymbol{N}_j = \overline{\sum_{\boldsymbol{j}}} \int \frac{|\psi_{j,l}(\boldsymbol{x})|^2}{\bar{n}_g(\boldsymbol{x})} d\boldsymbol{x}\,. \tag{8}$$

For the volume-limited survey, the noise power is simply $1/\bar{n}$.

Correct for the sampling effect by subtracting the shot noise term $N_{\boldsymbol{j}}$, and we have the estimator for banded power spectrum (Fang & Feng 2000),

$$\hat{P}_{\boldsymbol{j}} = I_{\boldsymbol{j}}^2 - \bar{N}_{\boldsymbol{j}}\,, \tag{9}$$

which is currently referred to as the DWT power spectrum.

4 TESTING THE DWT POWER SPECTRUM ESTIMATOR

In this section, we investigate the accuracy to which we are capable of recovering the DWT power spectrum from the mock PSCz galaxies using the methods described in the previous section.

4.1 Numerical Simulations

We consider three typical models each with ten realizations. The initial power spectrum is taken from the fitting formula given in Bardeen et al. (1986). The models are specified by the four parameters $(\Omega_0, \Lambda, \Gamma, \sigma_8)$, which are taken to be (1.0, 0.0, 0.5, 0.55) for the standard cold dark matter model (SCDM), (0.3, 0.7, 0.21, 0.85) for a low density flat model (ΛCDM) and (1.0, 0.0, 0.25, 0.55) for a variant of SCDM model (τCDM). We employ modified AP^{3}M code (Couchman 1991) to evolve 128^3 cold dark matter particles in a periodic cube of length $256\,h^{-1}$Mpc. Throughout our simulation process, for the mass assignment on the grid and the calculation of the force on a given particle from interpolation of the grid values, we use the triangular-shaped cloud (TSC) scheme. For the SCDM model, the starting redshift is taken to be $z_i = 15$, for LCDM and τCDM, $z_i = 25$. The force softening parameter η in the comoving system decreases with time as $\eta \propto 1/a(t)$. Its initial value is taken to be $\eta = 384\ h^{-1}$ kpc, and the minimum value to be $\eta_{\rm min} = 128\ h^{-1}$ kpc, corresponding to 15% and 5%, respectively, of the grid size. For the single-step integration of time evolution, we use the "leap-frog" scheme, the total number of integration steps down to $z = 0$ is 600.

4.2 Mock PSCz Galaxies

We construct PSCz mock catalogues from our N-body simulations. For simplicity, we assume that galaxies are unbiased tracers of the underlying mass distribution in the simulations. We apply the high-latitude PSCz sky mask to the simulations and replicate the periodic boxes where necessary to generate distant points. Then we generate flux-limited catalogues to the

maximum redshift $z_{\max} = 0.1$ using the parameterized selection function (Eq. (1)). The volume-limited catalogues are also generated by random sampling the mass points for a total number about equal to that of PSCz.

In comparison, we also consider the mock PSCz catalogues presented by Cole et al. (1998). Those catalogues were generated from a biased galaxy distribution, in which the biased galaxies were identified by a probability function of two-parameter selection in Lagrangian biased models. The parameters $(\Omega_0, \Lambda, \Gamma, \sigma_8)$ are (1.0, 0.0, 0.5, 0.55) for the standard CDM model (E4), (0.4, 0.0, 0.25, 0.95) for the low density open models(O4S) and low density flat model (0.3, 0.7, 0.25, 1.13) (L3S). For the detail of the method of constructing mock catalogues, refer to Cole et al. (1998).

From the flux-limited mock catalogues, we extract FLUX1 and FLUX2 subsets of the mock samples with selection criteria as described in Section 2. To perform the DWT power spectrum analysis, we put each sample inside a cuboid with sides $L_{\rm box} = 2r_{\max}$. The filling factor $f_s = \frac{V_{\rm s}}{L^3_{\rm box}}$(Yang et al. 2000) is estimated to be about 0.32, where $V_{\rm s}$ is the volume occupied by the sample. At a given scale j, there are $N_j = 2^{3j}$ perturbation modes $\tilde{\epsilon}_{j,\boldsymbol{l}}$, among which, obviously, only $f_s N_j$ modes contributes to the DWT power spectrum. To eliminate the discontinuity of the wavelet coefficients due to boundary effect, we distribute galaxies randomly in the empty regions (Poisson padding) with the same selection function as the PSCz galaxies.

Fig. 1 shows the real-space DWT power spectrum measured in the FLUX2 samples for each ensemble. The solid line in each panel shows the theoretical nonlinear DWT power spectrum of the model based on Eq. (5), in which the corresponding nonlinear Fourier power spectra are calculated using the Peacock & Dodds (1996) fitting formula. The filled squares in each panel show the DWT power spectrum averaged over 30 sub-samples, and the error bars are the standard 1σ deviations derived from their scatter. It is obvious that the filled squares are in good agreement with the theoretical nonlinear DWT power spectra at all the wavenumbers measured in $0.1h\,{\rm Mpc}^{-1} < k < 3h\,{\rm Mpc}^{-1}$. The relative DWT power spectrum fluctuations of SCDM and τCDM are larger than that of ΛCDM, but have comparable fluctuation powers due to the sparse sampling effect.

The DWT power spectra of FLUX1 samples are displayed in the left panel of Fig. 2. Again, we see a good agreement between the theoretical curves and the DWT power spectrum estimated in the mock samples at the wavenumbers $0.2 < k < 3h\,{\rm Mpc}^{-1}$. It is noted that the DWT power spectrum P_j at $j = 7$ is systematically underestimated. It comes about both from the shot noise term and from the limitation of spatial resolution in the simulations. We also analyzed the DWT power spectra of volume-limited samples in the right panels of Fig. 2. The VOLUME1 samples consist of about 1900 galaxies with a filling factor f_s of 0.38. As indicated in Fig. 2, the DWT power spectrum are basically consistent with the theoretical curves, but have larger error bars than those obtained from the FLUX1 samples. Actually, the VOLUME2 samples involve only about 1500 galaxies, which result in larger statistical fluctuations due to the sampling errors. In this case, the DWT spectrum estimates are too scattered to be statistically usable.

In Fig. 1 and Fig. 2, we have tested the DWT power spectrum estimator using the mock PSCz galaxies. The results show agreement between them in wavenumbers $0.1h\,{\rm Mpc}^{-1} < k < 3h\,{\rm Mpc}^{-1}$ resolved by the simulations. In comparison, we compute the DWT power spectra of mock PSCz catalogues based on the two-parameter Lagrangian biased Model(Cole et al. 1998). In Fig. 3, the DWT power spectrum measured in the flux-limited and volume-limited samples for the three models are shown in each panel as indicated in the figures. The dots, filled triangles, and filled squares represents those obtained from the FLUX1, FLUX2 and

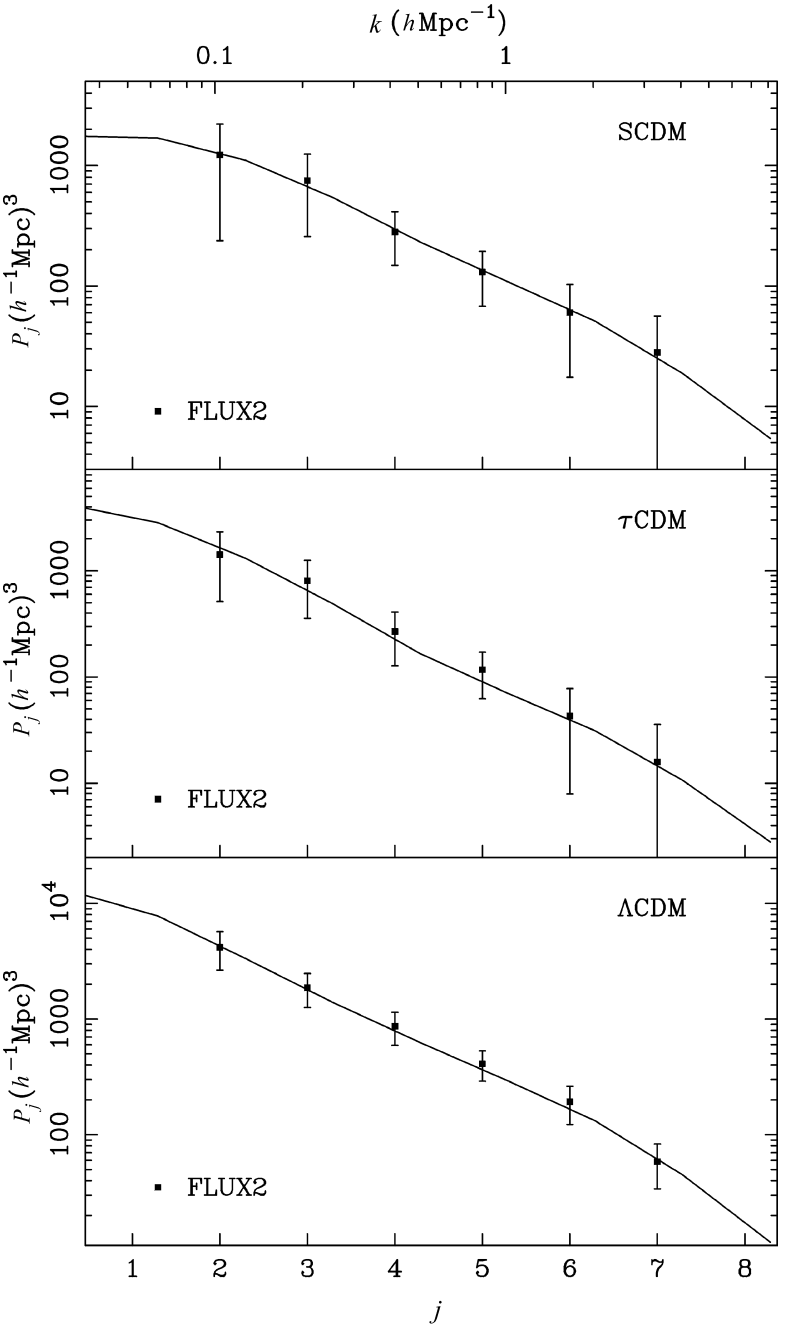

Fig. 1 The DWT power spectrum estimates of FLUX2 (see the text for more information) samples in real space. The solid line in each panel shows the theoretical nonlinear DWT power spectrum of the model. The filled squares are the mean DWT power spectrum estimates of 30 samples, and the error bars are the standard 1σ deviations derived from their scatters.

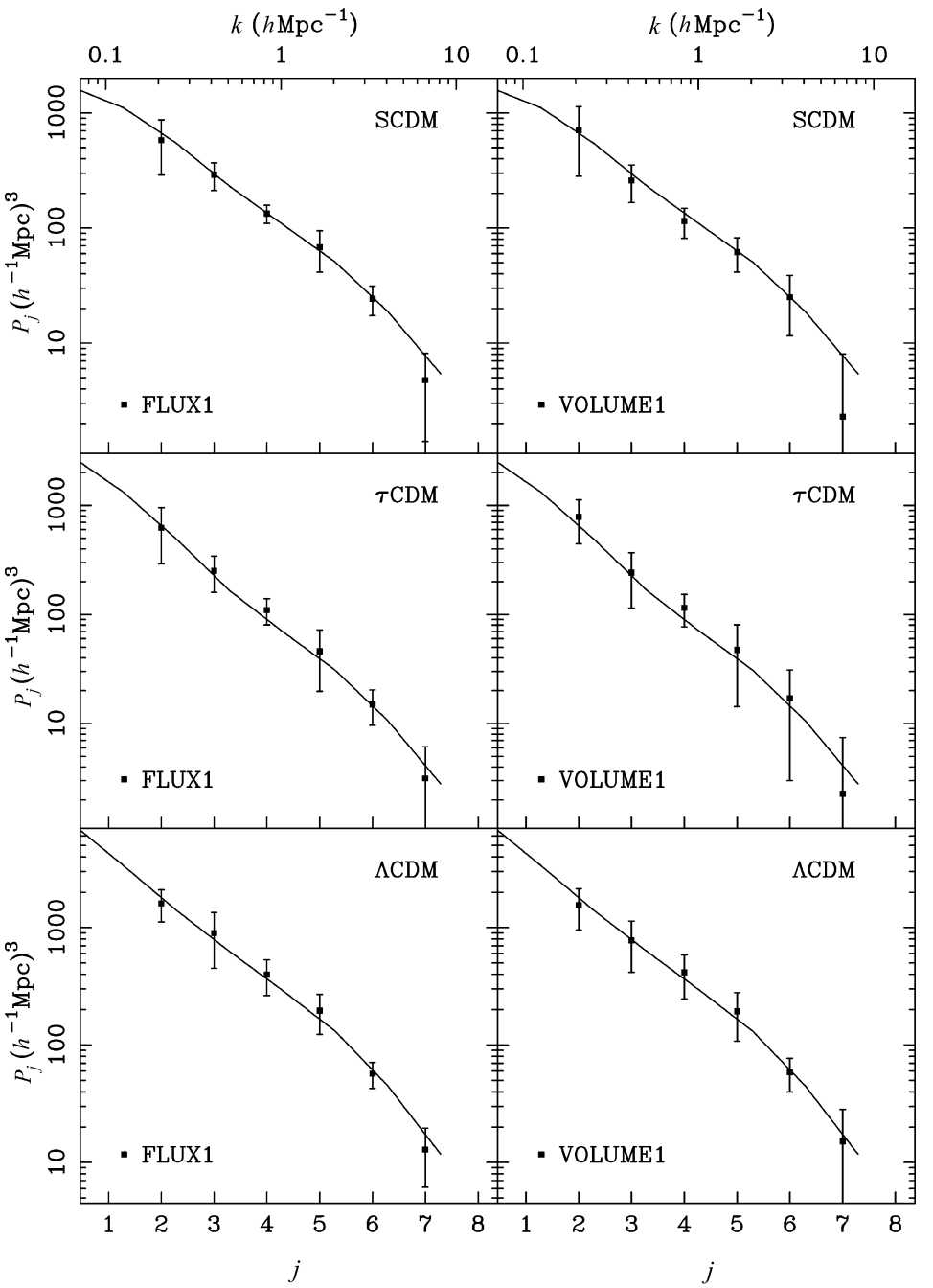

Fig. 2 The DWT power spectrum estimates of FLUX1 and VOLUME1 samples in real space. See keys in Fig. 1.

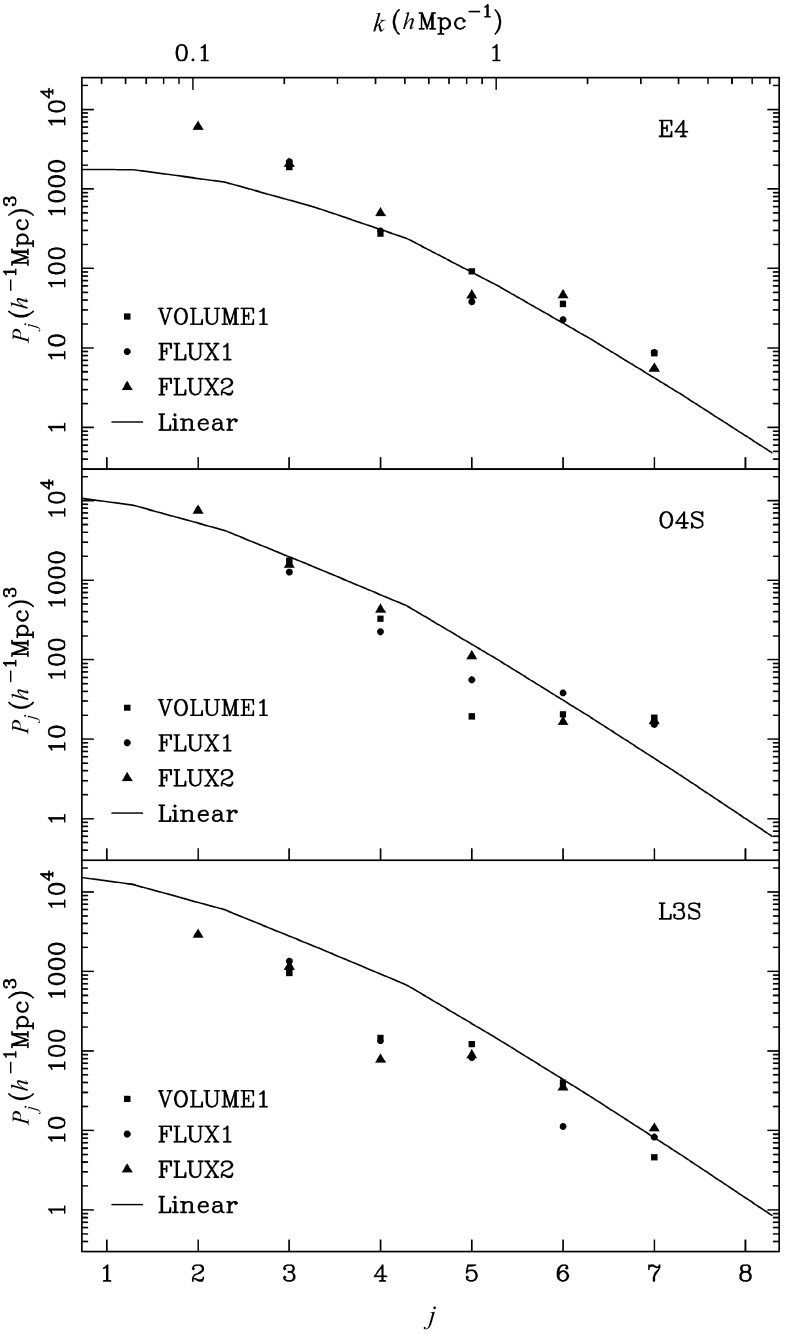

Fig. 3 The DWT power spectrum estimates of FLUX1 (dots), FLUX2 (filled triangles), VOLUME1 (filled squares) samples derived from mock PSCz catalogues of Cole et al. (1998). The solid line in each panel shows the theoretical linear DWT power spectrum. And the data are plotted according to the wavenumber.

VOLUME1 samples respectively. The solid line in each panel is the theoretical linear DWT power spectrum of each model. Because the spatial size of the FLUX2 is twice that of FLUX1 and VOLUME1, and the mode j corresponds to different wavenumbers, so we plot the data according to the wavenumbers. Apparently, Fig. 3 shows convergence of the estimations of DWT power spectra between the three kinds of samples. The DWT power spectra of biased galaxies deviate from those of the underlying mass in three ways, due to nonlinear evolution, bias and redshift distortions. Comparing with the linear power spectra, we find obvious bias or anti-bias effect in each model on the large scales. On the small scales, the amplitude is enhanced by the transfer of power from the large scales from nonlinear evolution. However, as indicated in Fig. 3. this effect is approximately canceled by the random motion of galaxies inside virialized groups and clusters of galaxies.

5 THE DWT POWER SPECTRUM OF THE PSCz

In this section, we analyze the DWT power spectra of PSCz galaxies. Fig. 4 shows the DWT power spectrum of the FLUX2 (filled triangles), FLUX1 (filled squares), and VOLUME1 (dots) samples of the PSCz catalogue. Obviously, the scatter of the DWT power spectra at the same wavenumbers is within the 1σ error bars of Fig. 1 and Fig. 2, which implies that the scatter is due to cosmic variance. It is emphasized here that the size of FLUX2 sample is different from those of FLUX1 and VOLUME1 samples. In this case, the DWT power spectrum estimated at the same wavenumbers are averaged over different modes. Their consistency further implies the reliability of the DWT power spectrum estimations.

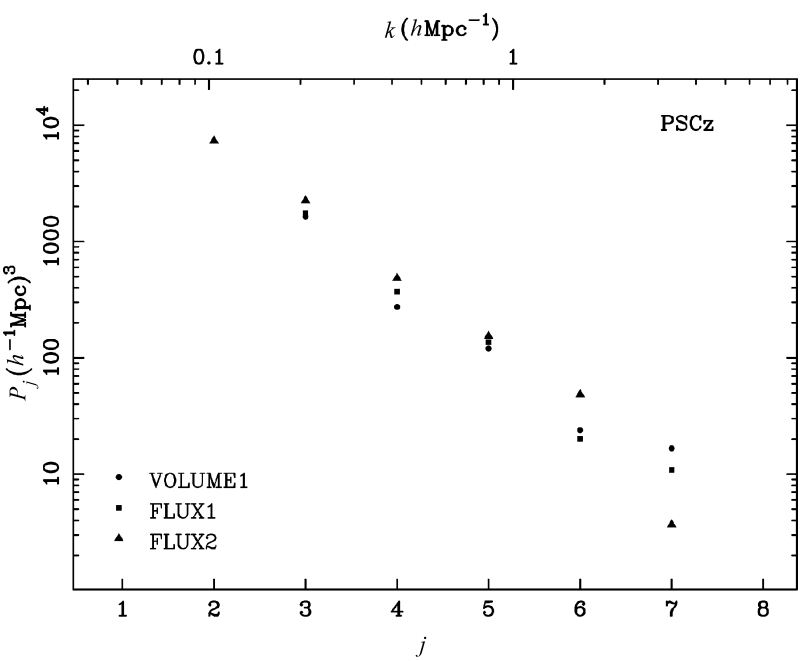

Fig. 4 The DWT power spectrum estimates of FLUX2 (filled triangles), FLUX1 (filled squares), and VOLUME1 (dots) samples of the PSCz catalogue.

Next we compare the DWT power spectrum of PSCz with theory and extract best-fitting values for the parameterized CDM models. For this, some assumptions are necessary,

(1) The power spectrum for the underlying matter distribution in the non-linear regime is assumed to be well modeled by the analytical fitting formulae given by Peacock & Dodds (1996), e.g., as plotted in Fig. 1.

(2) The fluctuations in the galaxy distribution are related to that of the dark matter distribution by $P_g(k) = b^2 P_m(k)$, where the biasing parameter b is simply assumed to be scale independent.

(3) The redshift distortion effect on the power spectrum due to the peculiar motion of galaxies in local gravitational fields can be quantified using the following formula (Peacock & Dodds 1994; Cole et al. 1995; Jing & Börner 2000):

$$P_{\rm s}(k) = b^2 P_{\rm m}(k)[1+\beta\mu^2]^2 D(\mu, k\sigma_v)\,, \tag{10}$$

where $P_{\rm s}(k)$ is the galaxy power spectrum in redshift space, $P_{\rm m}(k)$ the mass power spectrum in real space, $\beta = \Omega^{0.6}/b$, σ_v one dimensional velocity dispersion, μ the cosine of the angle between the wavevector and the line of sight, and the damping function $D(\mu, k\sigma_v)$ is given by

$$D(\mu, k\sigma_v) = (1 + k^2\sigma_v^2\mu^2/2)^{-2}\,, \tag{11}$$

in which the peculiar velocity on small scale has been assumed to have exponential distribution with one dimensional dispersion σ_v. The overall effect is obtained by averaging over μ (Cole et al. 1995).

The three CDM models are considered as reference fitting models. Besides the four parameters used for specifying the linear models, we fix the peculiar velocity dispersion σ_v and treat b as a free fitting parameter. The fitting DWT power spectra of PSCz with Eq. (10) are shown in Fig. 5, in which the 1-σ error bars placed on the observed DWT power spectrum are obtained from the mock samples for each CDM models. The best fitting parameters b for each model are listed in Table 1.

Table 1

Model	$b(1)$	$\beta(1)$	$\sigma_v(1)\,{\rm km\,s^{-1}}$	$b(2)$	$\beta(2)$	$\sigma_v(2)\,{\rm km\,s^{-1}}$
SCDM	1.33 ± 0.12	0.76 ± 0.07	300	1.89 ± 0.15	0.53 ± 0.04	600
τCDM	1.59 ± 0.13	0.63 ± 0.06	300	2.12 ± 0.16	0.47 ± 0.03	600
ΛCDM	0.95 ± 0.07	0.51 ± 0.04	300	1.17 ± 0.10	0.42 ± 0.04	600

The pairwise velocity dispersion is another important quantity measured in redshift surveys to characterize the clustering behavior on small scales. The early results obtained from the CfA-1 survey (Davis &Peebles 1983) gave a value of $v_{12}(\sim\sqrt{2}\sigma_v) \approx 340 \pm 40\,{\rm km\ s^{-1}}$ at a separation of $\sim 1h^{-1}$Mpc. As analyzed by Mo, Jing & Börner (1993), this estimate may be biased toward low values. The acceptable values are more likely to be within a wide range of 300–600 $\rm km\,s^{-1}$ (Hale-Sutton et al. 1989). The inferred value from the analysis of the CfA and Southern Sky Redshift Survey (Marzke et al. 1995) is about $v_{12} = 540 \pm 180\,{\rm km\,s^{-1}}$. The estimate based on the LCRS gives a comparable result $v_{12} = 570 \pm 80\,{\rm km\,s^{-1}}$ (Jing et al. 1998). In this paper, we adopt either the likely value of $\sigma_v = 300\,{\rm km\,s^{-1}}$ or the upper limit $\sigma_v = 600\,{\rm km\,s^{-1}}$ constrained by the observations.

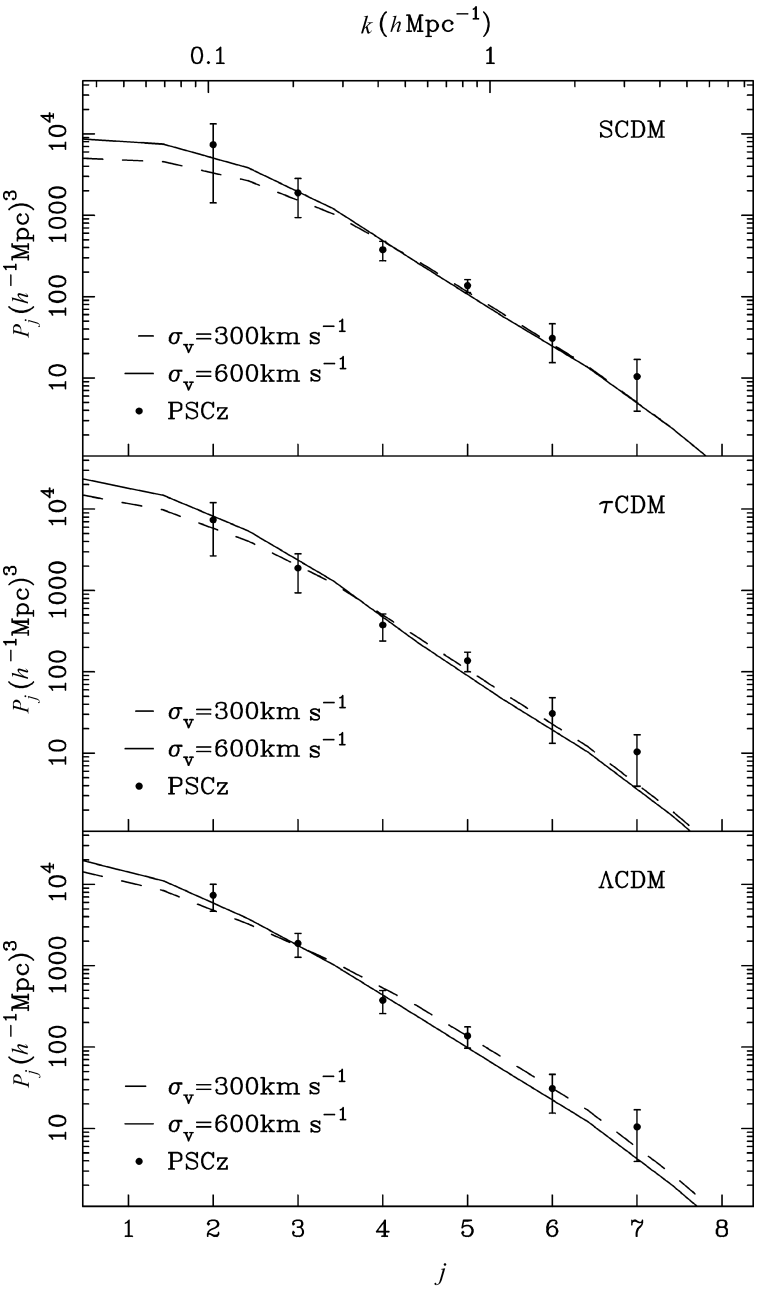

Fig. 5 The best-fitting (solid line) of the PSCz DWT power spectrum for models SCDM (upper panel), τCDM (central panel) and ΛCDM (lower panel) with the parameters listed in Table 1. The error bars are given by $1-\sigma$ variance obtained from the mock samples for each CDM model.

The τCDM and ΛCDM parameter β given in the Table 1 is consistent with other measurements, such as $\beta = 0.52 \pm 0.13$ for the 1.2 Jy IRAS survey by Cole et al. (1995) using angular harmonics of the power spectrum, $\beta = 0.47 \pm 0.16$ (Tadros et al. 1999) from a model-independent measurement using a maximum likelihood method in the PSCz. More recently, Hamilton et al. (2000) found a compatible result $\beta = 0.41^{+0.13}_{-0.12}$ by applying a combination of delicate analysis techniques. Moreover, we noted that our estimation of β in each of the three CDM models is very close to the corresponding linear β parameter $\sigma_8\Omega_0^{0.6}$. Assuming $\sigma_v = 300\,\mathrm{km\,s^{-1}}$, the amplitude of PSCz galaxy DWT power spectrum gives $b\sigma_8 = 0.73 \pm 0.07$ for SCDM and $b\sigma_8 = 0.81 \pm 0.06$ for ΛCDM, which is consistent with the value ~ 0.75 measured by Sutherland et al. (1999) using Fourier power spectrum analysis.

6 CONCLUSIONS

We conclude from the above discussion as follows,

(1) We tested the estimators of DWT power spectrum using mock catalogues constructed from N-body simulations in three typical CDM models. These tests show that the DWT power spectrum estimates are fairly stable and give small error bars on the scales we considered.

(2) We measured the DWT power spectrum of PSCz galaxies using flux limited samples and volume limited samples, which is then compared with those from the SCDM, τCDM and ΛCDM models including the effects of non-linear evolution of density perturbations and of redshift distortion. We estimated the redshift distortion parameter β using the least squares fitting for an assumed one-dimensional peculiar velocity dispersion σ_v.

(3) Comparing with different statistical analysis of the PSCz catalogue, we found that our DWT power spectrum analysis gives consistent results. It is impossible to distinguish different cosmic models at the present. Large redshift surveys of $10^5 - 10^6$ galaxies are required to determine the cosmology parameters accurately and give firm constraints.

Acknowledgements Supported by the National Natural Science Foundation of China.

References

Bardeen J. M., Bond J. R., Kaiser N., Szalay A. S., 1986, ApJ, 304, 15
Baugh C. M., Efstathiou G., 1993, MNRAS, 256, 154
Baugh C. M., Efstathiou G., 1994, MNRAS, 270, 183
Branchini E., Teodoro L., Frenk C. S. et al., 1999, MNRAS, 308, 1
Canavezes A., Springel V., Oliver S. J. et al., 1998, MNRAS, 297, 777
Cole S., Fisher K. B., Weinberg D. H., 1995, MNRAS, 275, 515
Cole S., Hatton S., Weinberg D. H., Frenk C. S., 1998, MNRAS, 300, 945
Couchman H. M. P., 1991, ApJ, 368, 23
Davies M., Peebles P. J. E., 1983, ApJ, 267, 465
Fang L. Z., Thews R., 1998, Wavelet in Physics, Singapore: World Scientific
Fang L. Z., Feng L. L., 2000, ApJ, 539, 9
Feldman H. A., Kaiser N., Peacock J. A., 1994, ApJ, 426, 23
Feng L. L., Chu Y. Q., Yang X. H., 2000, Acta Astrophys. Sinica, 20(3), 238
Fisher K. B., Davis M., Strauss M. A. et al., 1993, ApJ, 402, 42
Hale-Sutton D., Fong R., Metcalfe N., Shanks T., 1989, MNRAS, 237, 569
Hamilton A. J. S., Tegmark M., Padmanabhan N., 2000, astro-ph/0004334
Jing Y. P., Börner G., 2000, astro-ph/0009032

Jing Y. P., Mo H. J., Börner G., 1998, ApJ, 494, 1
Lin H., Kirshner P., Shectman S. A. et al., 1996, ApJ, 471, 617
Marzke R. O., Geller M. J., da Costa L. N., Huchra J. P., 1995, AJ, 110, 477
Mo H. J., Jing Y. P., Börner G., 1993, MNRAS, 264, 825
Pando J., Fang L. Z., 1998, Phys. Rev., E57, 3593
Park C., Vogeley M. S., Geller M. J., Huchra J. P., 1994, ApJ, 431, 569
Peacock J. A., Dodds S. J., 1994, MNRAS, 267, 1020
Peacock J. A., Dodds S. J., 1996, MNRAS, 280, L19
Rowan-Robinson M., Sharpe J., Oliver S. J. et al., 2000, MNRAS, 314, 375
Saunders W. et al., 2000, MNRAS, 317, 55
Sutherland W., Tadros H., Efstathiou G. et al., 1999, MNRAS, 308, 289
Tados H., Efstathiou G., 1996, MNRAS, 282, 1381
Tadros H., Ballinger W. E., Taylor A. N. et al., 1999, MNRAS, 305, 527
Yang X. H., Feng L. L., Chu Y. Q., Fang L. Z., 2000, ApJ, 553, 1